Modelling river-bank-erosion processes and mass failure mechanisms: progress towards fully coupled simulations

Gravel-Bed Rivers VI: From Process Understanding to River Restoration
H. Habersack, H. Piégay, M. Rinaldi, Editors

9

Modelling river-bank-erosion processes and mass failure mechanisms: progress towards fully coupled simulations

Massimo Rinaldi and Stephen E. Darby

Abstract

This paper reviews recent developments in modelling the two main sets of bank-erosion processes and mechanisms, namely fluvial erosion and mass failure, before suggesting an avenue for research to make further progress in the future. Our review of mass failure mechanisms reveals that the traditional use of limit equilibrium methods to analyse bank stability has in recent years been supplemented by research that has made progress in understanding and modelling the role of positive and negative pore water pressures, confining river pressures, and hydrograph characteristics. While understanding of both fluvial erosion and mass failure processes has improved in recent years, we identify a key limitation in that few studies have examined the nature of the interaction between these processes. We argue that such interactions are likely to be important in gravel-bed rivers and present new simulations in which fluvial erosion, pore water pressure, and limit equilibrium stability models are combined into a fully coupled analysis. The results suggest that existing conceptual models, which describe how bank materials are delivered to the fluvial sediment transfer system, may need to be revised to account for the unforeseen effects introduced by feedback between the interacting processes.

1. Introduction

Bank erosion is a key process in fluvial dynamics, affecting a wide range of physical, ecological, and socio-economic issues in the fluvial environment. These include the establishment and evolution of river and floodplain morphology and their associated habitats (e.g., Hooke, 1980; Millar and Quick, 1993; Darby and Thorne, 1996a; Barker et al., 1997; Millar, 2000; Goodson et al., 2002), turbidity problems (e.g., Bull, 1997; Eaton et al., 2004), sediment, nutrient, and contaminant dynamics (e.g., Reneau et al., 2004), loss of riparian lands (e.g., Amiri-Tokaldany et al., 2003), and associated threats to flood defence and transportation infrastructure (e.g., Simon,

E-mail address: mrinaldi@dicea.unifi.it (M. Rinaldi)

ISSN: 0928-2025 DOI: 10.1016/S0928-2025(07)11126-3

1995). Moreover, recent studies have shown that the contribution of bank-derived sediments to catchment sediment budgets may be higher than previously thought, although the precise fraction varies depending on the time-scale of measurement (Bull, 1997). For example, considering annual sediment yields, Walling et al. (1999) showed that bank sediments contribute up to 37% of the total (10,816 t/yr) suspended sediment yield, even in the relatively low-energy catchments of the UK, with the contribution rising to values as high as 80% of the total (75,000 t/yr) suspended sediment yield in some highly unstable, incised, channel systems (e.g., Simon and Darby, 2002). With such a significant fraction of material within the alluvial sediment system derived from river banks, it is evident that knowledge of the rates, patterns, and controls on bank-erosion events that release sediment to river systems is a pre-requisite for a complete understanding of the fluvial sediment transport regime.

Naturally, much research has already been devoted to these issues. These contributions include a number of excellent reviews (Lawler, 1993; Lawler et al., 1997b; Couper, 2004), including those published by Grissinger (1982) and Thorne (1982) in the original *Gravel-Bed Rivers* volume (Hey et al., 1982). So what might 'yet' another review of bank-erosion processes actually achieve? As Fig. 9.1 shows, there is a growing number of bank-erosion investigations (38% of the publications appear after 1997) and a shift in the pattern of 'hot' topics in the discipline. In particular, new research has elucidated the role of riparian vegetation (e.g., Abernethy and

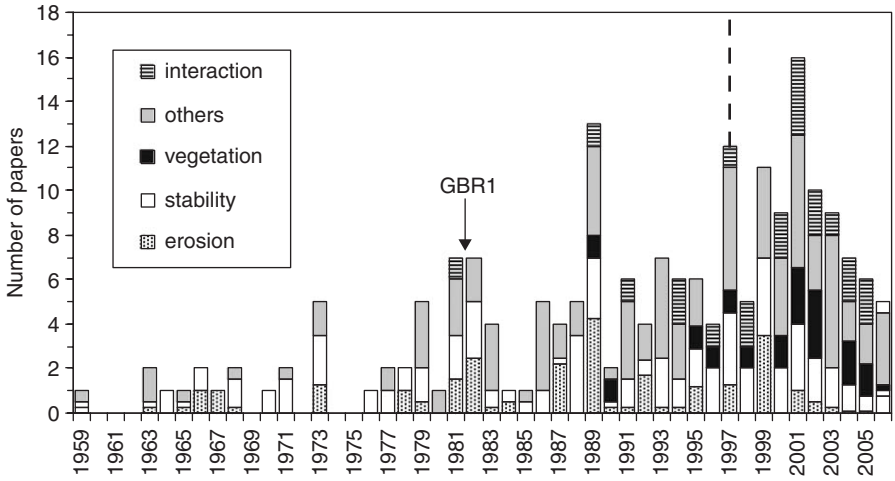

Figure 9.1. Summary of the bibliographic review on river-bank-erosion processes conducted for this chapter (total of 194 papers considered). Erosion: papers focused on fluvial entrainment; stability: papers on mass failures and bank stability; vegetation: papers focusing on the role of vegetation; others: papers on other issues related to bank erosion (e.g., measurement of bank retreat, variables controlling rates of retreat, sediment delivery from bank processes, influence of bank processes on channel geometry, etc.); interaction: papers on modelling width adjustments and channel migration, and including to some extent the interaction between fluvial erosion and mass failures. Dates of major reviews of bank erosion in the first *Gravel-Bed Rivers I* proceedings volume in 1982 (GBR I) and the most recent major review in 1997 (dashed line) are also highlighted.

Rutherfurd, 1998, 2000; Simon and Collison, 2002) and bank hydrology (e.g., Rinaldi and Casagli, 1999; Casagli et al., 1999; Rinaldi et al., 2004) as key controlling influences on bank stability. In contrast, although improvements in the modelling of near-bank flows are starting to be made (e.g., Kean and Smith, 2006a,b), there are still relatively few studies that have been concerned with the process of fluvial erosion (i.e., the removal of bank sediments by the direct action of the flow). Accordingly, little progress has been made in understanding fluvial bank erosion of cohesive sediments since the contributions of Arulanandan et al. (1980) and Grissinger (1982). Notable exceptions to this trend include some work that has sought to quantify entrainment thresholds and process rates (e.g., Lawler et al., 1997a; Simon et al., 2000; Dapporto, 2001). The role of weathering as a significant agent of erosion has also started to be recognised (e.g., Lawler, 1993; Prosser et al., 2000; Couper and Maddock, 2001), both in headwater reaches (where weathering may be the dominant mechanism by which sediment is removed from the bank face) and, elsewhere, as a mechanism for enhancing bank erodibility and promoting fluvial erosion.

Fig. 9.1 also highlights another gap in the literature. While most studies recognise that bank retreat is the integrated product of three interacting processes (namely, weathering and weakening, fluvial erosion, and mass failure), they tend to adopt reductionist approaches that focus on a single set of processes, so interactions between different groups of processes are not usually considered. This is important because dynamic interactions and feedbacks between processes may lead to outcomes that are not predictable a priori. In short, viewing bank processes in isolation is unrealistic and introduces the possibility that conclusions derived from such studies are biased.

Recognition of this problem is not new. Lawler (1992) introduced a conceptual model of changing bank process dominance in a hypothetical drainage basin (Fig. 9.2), emphasising that processes act not in isolation, but are always present to a varying degree. While Fig. 9.2 represents a conceptualisation of an idealised basin and the length scales therein are, therefore, deliberately omitted, it is instructive to attempt to contextualise the drainage basin locations within which recent bank-erosion research has been conducted. Bearing in mind that these studies have typically sought to isolate the effects of individual process groups, it is noteworthy that they cluster in the mid- to downstream reaches, where process interactions are strongest. Interactions between mass failure and fluvial-erosion processes (as opposed to the role of individual processes acting in isolation) therefore have particular relevance in the context of gravel-bed rivers, as the zone of interaction coincides at least in part with the middle reaches of basins where gravel-beds are typical, and also because the dominance of subaerial processes is generally limited geographically to the headwaters of typical fluvial systems (Couper and Maddock, 2001).

This paper therefore seeks to address two objectives. First, we review recent developments regarding the two main bank-erosion phenomena (fluvial erosion and mass failure) responsible for bank retreat in gravel-bed rivers. Second, we focus on studies which have sought to address the interactions between these two processes and mechanisms. Included in this synthesis are new findings from our own research which show that adopting a fully coupled modelling approach that views bank processes as interacting, rather than individual, entities leads to a distinctive vision of

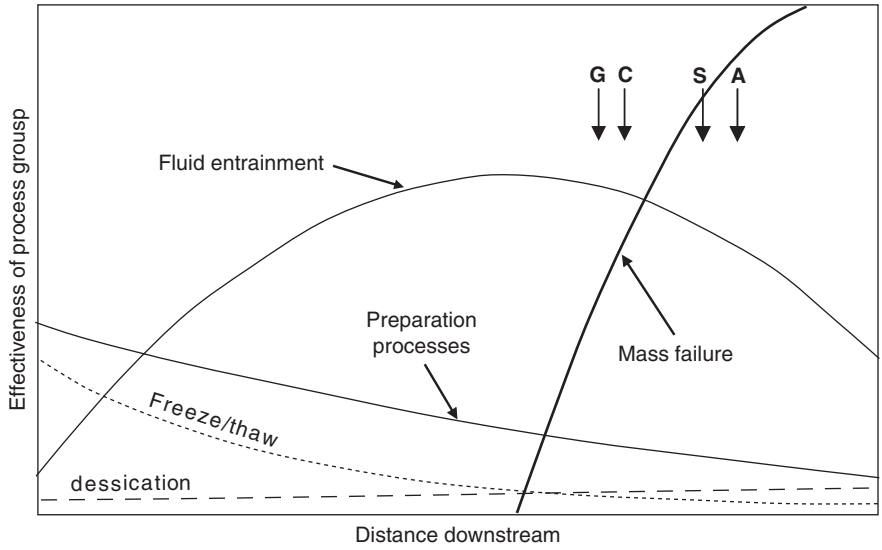

Figure 9.2. Conceptual model of process dominance in the fluvial system. (After Lawler (1992)). Also shown are the approximate locations within their respective basins (mapped as proportion of stream length) of the sites used in some recent bank-erosion studies: A = River Asker, Dorset, UK; C = Cecina River, Tuscany, Italy; G = Goodwin Creek, Mississippi, USA; S = Sieve River, Tuscany, Italy. (Reproduced with permission from Wiley and Sons, 1992.)

the ways in which bank-derived materials are delivered to the alluvial sediment transfer system.

2. Modelling fluvial erosion

Fluvial erosion is defined as the removal of bank material by the action of hydraulic forces, although it generally occurs in combination with weathering processes that prepare bank sediments for erosion by enhancing their erodibility (Hooke, 1980; Thorne, 1982; Lawler, 1993; ASCE Task Committee on Hydraulics, Bank Mechanics, and Modeling of River Width Adjustment, 1998; Prosser et al., 2000; Couper and Maddock, 2001). Relative to mass failure, fluvial erosion is, at the scale of the flow event and once the critical entrainment threshold has been exceeded, a quasi-continuous process, with the volume of sediment delivered by fluvial erosion dependent on the duration of the competent flow. In general, fluvial-erosion rates depend on the near-bank flow intensity and physical characteristics (i.e., the erodibility) of the bank material. However, this simple conceptualisation masks enormous complexity that results from the inherent variability of the relevant controlling parameters. Thus, observed rates of fluvial-erosion range over several orders of magnitude (Hooke, 1980) and fluvial-erosion rates are predictable only to the extent that the controlling parameter values, and their inherent variability, can be estimated accurately.

It is widely accepted that the rate of fluvial bank erosion can be quantified using an excess shear stress formula such as (Partheniades, 1965; Arulanandan et al., 1980):

$$\varepsilon = k_{\mathrm{d}}(\tau - \tau_{\mathrm{c}})^{a} \tag{9.1}$$

where ε (m/s) is the fluvial bank-erosion rate per unit time and unit bank area, τ (Pa) is the boundary shear stress applied by the flow, k_{d} ($\mathrm{m^2s/kg}$) and τ_{c} (Pa) are erodibility parameters (erodibility coefficient, k_{d}, and critical shear stress, τ_{c}), and a (dimensionless) is an empirically derived exponent. It is important to note that although excess shear stress models of this type are widely accepted and used in a range of geomorphological applications (e.g., Arulanandan et al., 1980; Govers, 1991; Howard, 1994), no formal validation of this model has yet been undertaken. Thus some uncertainty remains over the value of the exponent a (which is commonly assumed to take a value close to 1 for most studies involving cohesive sediments, e.g., Partheniades, 1965).

Perhaps more significantly, the physical basis of the excess shear stress model for bank erosion can be questioned. One problem is its reliance on a threshold value, which is difficult to incorporate into numerical models due to the sharp threshold between stability and failure, which in turn results in instabilities near the threshold value. Nevertheless, such threshold behaviour is appropriate, particularly on cohesive river banks. Any propagation of numerical error may, therefore, de facto require the erodibility coefficient (k_{d}) to be treated as a calibration parameter, a problem highlighted recently by Crosato (2007).

For the purposes of this review we assume that the basic form of equation (9.1) is robust and that predictive ability is limited by the need to estimate the necessary parameter values accurately. In subsequent sub-sections we therefore focus on recent developments concerned with improving estimates of the erosion rate, erodibility, and shear stress parameters.

2.1. Erosion rate

A comprehensive review of the methods used to observe bank erosion was provided by Lawler (1993). Recently, techniques such as digital photogrammetry and laser scanning (e.g., Lane et al., 1994; Barker et al., 1997; Nagihara et al., 2004) can provide the opportunity to define river bank topography at unprecedented spatial resolution (surveys with point densities of ca. 10^7 points across a bank face are readily obtainable using terrestrial laser scanning) and accuracy (± 2 mm). Bank erosion can then be quantified using the survey data to construct Digital Terrain Models (DTMs) for time intervals and differencing to establish net change. However, logistical and safety concerns usually limit the frequency of monitoring to relatively coarse timescales, at best perhaps resolving individual flow events. This is problematic because the pre- versus post-*flow* event 'window' is not the same thing as the *bank erosion* event window, such that it is not usually possible to resolve process thresholds, timing, and rates (Lawler, 2005). To address this limitation, new quasi-continuous bank-erosion sensors based on the use of photoelectronic cells (PEEPs; e.g., Lawler, 1993; Lawler et al., 1997a) and thermal consonance timing (TCT; e.g., Lawler, 2005) have been

developed, though they have not yet been widely deployed. While these approaches are promising, the use of sensors can disturb the bank face, while excellent temporal resolution is inevitably obtained at relatively low spatial resolution. While accurate and representative discrimination of bank-erosion rates therefore remains elusive, studies that combine high spatial/low temporal (e.g., photogrammetry) and high temporal/low spatial (e.g., PEEPs, TCT) resolution approaches may deliver exciting new results in the near future.

2.2. *Erodibility of bank sediment*

For granular (non-cohesive) sediments, bank erodibility parameters are modelled based on the same methods that are used to predict the entrainment of bed sediments, albeit with modifications to take into account the effect of the bank angle on the downslope component of the particle weight (Lane, 1955) and the case of partly packed and cemented sediments (e.g., Millar and Quick, 1993; Millar, 2000). Determination of critical shear stress for cohesive materials is more complex, given that it is widely recognised that fluvial entrainment for cohesive sediments depends on several factors, including (amongst others) clay and organic content, and the composition of interstitial fluids (Arulanandan et al., 1980; Grissinger, 1982; Knapen et al., 2007). Consequently methods for predicting the erodibility of cohesive banks remain poor.

To address this issue, recent studies have deployed in situ jet-testing devices (e.g., Hanson, 1990; Hanson and Simon, 2001) to obtain direct measurements of bank erodibility (e.g., Dapporto, 2001). This is achieved by directing a jet of water with known hydraulic properties at the bank material. The resulting deformation is measured periodically with a mechanical point gauge, until an equilibrium scour depth is attained. The measured deformation rate, scour depth, and known hydraulic properties are used to determine the erodibility parameters. While jet-testers offer in situ sampling, our experience is that their design (especially their large weight) makes their deployment to inaccessible sites difficult, and it is also hard to emplace them without disturbing the bank surface. Moreover, individual tests are time consuming (ca. 0.5 h), making it difficult to obtain the numbers of samples needed to adequately characterise the spatial and temporal variability of the bank materials. On resistant surfaces, errors involved in mechanically inserting the point gauge into the base of the scour hole can be similar in magnitude to the scour depth itself, while erodible materials generate scour depths that can exceed the extent of the gauge.

Instruments such as the Cohesive Strength Meter (Tolhurst et al., 1999) appear to offer advantages over conventional jet-testing devices. The CSM is similar to these in that water jets of increasing strength are directed at the target surface. However, instead of measuring the resulting scour depth, the CSM detects erosion by monitoring optical transmission in an enclosed sampling head chamber. Thus, the moment of erosion corresponds to sudden reductions in optical transmission induced by the suspension of eroded sediment within the test chamber, with the jet properties at that threshold defining the critical stress. Tests are both automated and rapid (<3 min) so the device can easily be used to obtain large numbers of samples. So far

it has only been deployed in estuarine environments (Tolhurst et al., 1999), but the CSM appears to offer a potentially fruitful avenue of bank-erosion research.

2.3. Near-bank shear stresses

With the aforementioned recent developments in bank-erosion monitoring technology and in the quantification of bank erodibility, the 'missing link' in equation (9.1) remains the difficulty of characterising the fluid stresses that are exerted on river banks during the large flows that typically drive erosion. Bank boundary shear stress is highly variable both in space and time, dependent as it is on such factors as the bank geometry (which is itself highly variable), cross-section size and shape, channel curvature, and flow stage. This variability presents a challenge for anyone seeking to characterise the shear stress distribution via direct measurement. Sampling strategies would need to capture this natural variability, suggesting that the necessary flow velocimetry equipment would need to be deployed at high spatial and temporal resolution, during the (hazardous) high flow conditions associated with bank erosion. It is, therefore, unsurprising that such investigations are lacking, apart from some flume studies (e.g., Blanckaert and Graf, 2001) which are able to achieve the necessary sampling resolution, albeit under rather idealised conditions.

If field data collection is impractical, the only viable alternative is to predict the shear stress values using hydraulic models. Some models have been developed using empirical data sets obtained from laboratory channels (Leutheusser, 1963; Kartha and Leutheusser, 1972; Simons and Sentürk, 1977; Knight et al., 1984), but these can only be applied with caution to natural rivers, as the bank and channel forms present in flumes with regular geometry represent the problem rather poorly. Recently, progress has been made in using analytical models to quantify form roughness induced by the irregular bank morphology and partition the shear stress acting on the banks (e.g., Kean and Smith, 2004, 2006a,b; Griffin et al., 2005). Although these approaches are promising, it is not yet clear whether such approaches are entirely appropriate. Specifically, a lack of field data sets means that we simply do not yet know whether near-bank flows are dominated by the form drag induced by the topographic irregularities (e.g., embayments, slump deposits, etc.) associated with natural, eroding, banks (e.g., Thorne and Furbish, 1995), or by the effects of turbulence induced by strong lateral shear and the occurrence of wakes. If the latter is the case, then modelling near-bank flows would require the application of 3-dimensional Computational Fluid Dynamics (3D-CFD) modelling techniques.

The practice of using 3D-CFD modelling techniques as a substitute for field data in river flows that are difficult or impossible to measure has now become established for a range of open-channel flow contexts (e.g., Nicholas and Walling, 1997, 1998; Hodskinson and Ferguson, 1998; Nicholas and Sambrook-Smith, 1999; Bradbrook et al., 2000; Lane et al., 2000; Darby et al., 2004). However, the application of 3D-CFD to near-bank flows remains novel and replication of near-bank flows would depend on: (i) ensuring the discretised computational scheme accurately solves the underlying conservation equations; (ii) selecting an appropriate turbulence-closure model (TCM), and (iii) accurately defining the initial and boundary conditions

(Darby et al., 2004). Accepted standards of computational mesh design (e.g., American Society of Mechanical Engineers (ASME), 1993; American Institute of Aeronautics and Astronautics (AIAA), 1998) are already available, with adherence to those standards ensuring that discretisation and numerical solution errors are minimised (Hardy et al., 2003). Consequently, we focus attention on the latter two issues, though we note that very high-resolution grids are likely to be needed to represent the complex flow structures in near-bank environments. This, in turn, may create additional problems, not only of large computational requirements, but in terms of defining the boundary conditions correctly. Regarding the parameterisation of turbulence, some studies have begun to investigate the potential for approaches such as Direct Numerical Simulation (DNS) and Large Eddy Simulation (LES) to deliver accurate hydraulic data (e.g., Rodi et al., 1997). However, even with the capabilities of modern computing, these approaches have only been applied to flows with fixed (non-deformable) channel boundaries. For morphological modelling, Reynolds averaging appears set to continue as the only feasible approach, at least for the foreseeable future. However, all such TCMs contain empirical elements, so model selection must be matched to the anticipated physical conditions, namely: (i) strong lateral shear; (ii) occurrence of separated flow around topographic irregularities (e.g., embayments, slump deposits, etc.) associated with eroding banks. These requirements suggests that an anisotropic TCM is required (e.g., So et al., 1993; Sotiropoulos, 2001; Blanckaert and Graf, 2001; Gerolymos et al., 2002), and a Reynolds Stress Model (RSM) appears most appropriate for the specific context of modelling near-bank flows.

3. Modelling river bank failures

Mass failure is the collapse and movement of bank material under gravity. Relative to fluvial erosion, mass failure is discontinuous and large-scale and occurs by any of a number of mechanisms (Thorne, 1982), with a specific model required for each. The methods developed and used in the literature have concentrated only on a relatively few of these, in particular slides (planar or rotational) and cantilever failures. Referring to the classical mechanism of a planar slide (Lohnes and Handy, 1968), bank failure occurs when the destabilising forces, due to gravity, exceed the resisting forces, which are related to the shear strength of the bank materials expressed by the failure criterion of Fredlund et al. (1978) as:

$$\tau = c' + (\sigma - u_a)\tan\phi' + (u_a - u_w)\tan\phi^b \tag{9.2}$$

where τ is the shear strength (kPa), c' the effective cohesion (kPa), σ the normal stress (kPa), u_a the pore air pressure (kPa), ϕ' the friction angle in terms of effective stress (°), u_w the pore water pressure (kPa), (u_a–u_w) the matric suction (kPa), ϕ^b the angle expressing the rate of increase in strength relative to the matric suction (°). In saturated conditions, the apparent cohesion (the third term on the right-hand side of

equation (9.2) disappears so equation (9.2) reduces to the classical Mohr–Coulomb criterion.

3.1. Methods of analysis

The application of stability analyses is common in the bank-erosion literature. The analysis of slide failures is typically performed using a Limit Equilibrium Method (LEM) to compute the factor of safety (F), defined as the ratio between stabilising and destabilising forces. Since the 1960s, specific methods of bank stability analysis have been progressively disseminated, with an increasing effort to define closed-form solutions for planar failures representative of characteristic bank geometries (Table 9.1). It is evident that research has progressively sought to account for: (1) a more realistic bank geometry and the influence of tension cracks (Osman and Thorne, 1988); (2) positive pore water pressures and hydrostatic confining pressures (Simon et al., 1991; Darby and Thorne, 1996b); (3) the effects of negative pore water pressures in the unsaturated part of the bank (Rinaldi and Casagli, 1999; Casagli et al., 1999; Simon et al., 2000); and (4) the influence of riparian vegetation (Abernethy and Rutherfurd, 1998, 2000, 2001; Simon and Collison, 2002; Rutherfurd and Grove, 2004; Pollen et al., 2004; Van de Wiel and Darby, 2004; Pollen and Simon, 2005; Pollen, 2006).

Recently, more complex analyses have been utilised for river bank studies (Abernethy and Rutherfurd, 2000; Dapporto et al., 2001, 2003; Simon et al., 2002; Rinaldi et al., 2004) by using various LEM solutions extended to rotational slides (i.e., Bishop, Fellenius, Jambu, Morgestern, GLE) that include features that overcome many of the previous limitations. These analyses provide the following advantages: (1) rotational or composite slide surfaces and generic bank geometries can be defined; (2) either the Mohr–Coulomb or Fredlund et al. (1978) failure criterion can be selected depending on whether the soil conditions are saturated or unsaturated, respectively; (3) a generic pore water pressure distribution can be defined, and confining pressures due to the river can be accounted for; (4) it is possible to perform several analyses for a large number of different sliding surface types and positions, providing more confidence in the identification of the most critical failure surface.

On the other hand, it is important to recognise that LEM analyses also have some important limitations (Duncan and Wright, 2005). The main one is probably the fact that the mass delimited by the sliding surface is assumed to not be subject to deformation. In other words, only the stresses along the failure surface are accounted for, not the stress distribution within the soil mass. In order to characterise this deformation processes, more complex and sophisticated models used for slope analyses, namely stress-deformation analysis, are required (Griffiths and Lane, 1999; Collison, 2001). Such models have not yet been employed specifically for riverbanks, due to some main reasons: (1) stress-deformation analyses are particularly data-demanding and complex to use; (2) riverbank failures typically occur rapidly, whereas stress-deformation analyses are typically applied to slow landslides, deep-seated deformation, and/or progressive failures on large slopes (e.g., Wiberg et al., 2005; Hürlimann et al., 2006).

Table 9.1. Summary of methods of stability analysis applied to river banks.

Analysis	Mechanism of failure and bank geometry	New capabilities (compared to previous methods)	Main limitations	Typical applications	Main references
'Culmann'	Planar failure, uniform bank slope	Simple to use	Simplified geometry; failure surface passing from the bank toe; pore water pressures not included	Massive silt or clay, incised rivers of southeastern – midwestern U.S.	Thorne et al. (1981); Thorne (1982)
Thorne & Tovey	Cantilever failure	First method specific for cantilever failure	Data required not easily available	Composite banks	Thorne and Tovey (1981); Thorne (1982); Van Eerdt (1985)
Osman & Thorne (O&T)	Planar failure with tension crack; bank profile taking into account basal erosion and relic tension crack	More realistic geometry including effects of basal erosion	Failure surface passing from the bank toe; pore water pressures not included	Homogeneous, steep, cohesive banks	Osman and Thorne (1988); Thorne and Abt (1993)
Simon et al.	Planar failure, uniform bank slope	Failure surface not passing from the bank toe; positive pore pressures and confining pressures incorporated	Simplified bank geometry (no tension crack)	Homogeneous, steep, cohesive banks	Simon et al. (1991)

Darby & Thorne	Planar failure with vertical tension crack, O&T geometry	More realistic geometry with positive pore pressures and confining pressures incorporated	Unsaturated conditions are not considered	Homogeneous, steep, cohesive banks	Darby and Thorne (1996b)
Rinaldi & Casagli	Planar failure with vertical tension crack, uniform bank slope	Negative pore water pressures taken into account	Simplified bank geometry; simplified assumptions on water table during drawdown	River banks formed in partially saturated soils; rivers with relatively rapid drawdown	Rinaldi and Casagli (1999)
Casagli et al.	Planar failure with vertical tension crack, O&T geometry	More realistic geometry	Homogeneous material; Relation river stage – water table needs to be specified	Homogeneous, steep, cohesive river banks formed in partially saturated soils	Casagli et al. (1999), Rinaldi and Casagli (1999)
Simon et al.	Planar failure with vertical tension crack, O&T geometry	Layered bank materials	Relation river stage – water table needs to be specified	Layered cohesive river banks formed in partially saturated soils	Simon et al. (2000)
USDA Bank stability model	Planar (wedge-type) failure	Incorporates soil reinforcement and surcharge due to vegetation	Simplified bank geometry	Vegetated river banks	Simon and Collison (2002)
Various commercial software packages	Slides (planar, rotational, composite); generic bank geometry	Generic bank geometry and failure surfaces; possible to account for main vegetative mechanical effects	Generally more data-demanding; requires expertise	When pore water pressure changes at the intra-event scale need to be accounted; rotational or other non-planar failure surfaces and generic bank geometry	Dapporto et al. (2001, 2003); Rinaldi et al. (2004)

3.2. *Effects of pore water pressures*

Changes in pore water content and pressures are recognised as one of the most important factors controlling the onset and timing of bank instability (Thorne, 1982; Springer et al., 1985) and the incorporation of these factors in bank process models is one of the major areas of recent progress. Pore water has at least four main effects: (1) reducing shear strength; (2) increasing the unit weight of the bank material; (3) providing an additional destabilising force due to the presence of water in tension cracks (i.e., the force of the water on the sides of the cracks before it infiltrates into the soil material); (4) providing additional (stabilising or destabilising) seepage forces.

A crucial point when accounting for pore water pressures is their extremely transient character, driven as they are by dynamic hydrological variables (rainfall, river hydrograph). The actual mechanisms and timing of failure induced by pore water pressure effects are difficult to predict if their temporal changes, both at seasonal and intra-event time scales, are not accounted for (Rinaldi and Casagli, 1999; Casagli et al., 1999; Simon et al., 2000). For this reason, bank stability response at the intra-event time scale requires knowledge of the dynamics of saturated and unsaturated seepage flows. Various studies (Dapporto et al., 2001, 2003; Rinaldi et al., 2001, 2004) have made use of the software Seep/w (Geo-Slope International Ltd) to perform two-dimensional, finite element seepage analyses (Fig. 9.3A) based on the mass conservation equation in a form extended to unsaturated conditions (Fredlund and Rahardjo, 1993):

$$\frac{\partial}{\partial x}\left(k_x \frac{\partial H}{\partial x}\right) + \frac{\partial}{\partial y}\left(k_y \frac{\partial H}{\partial y}\right) + Q = \frac{\partial \theta}{\partial t} \tag{9.3}$$

where H is the total head (m), k_x the hydraulic conductivity in the x-direction (m/s), k_y the hydraulic conductivity in the y-direction (m/s), Q the unit flux passing in or out of an elementary cube (in this case an elementary square, given that the equation is in two-dimensions) (m^2/m^2s), θ the volumetric water content (m^3/m^3), t the time (s). Positive and negative pore water pressure distributions obtained by the seepage analysis are then used as input data for the stability analysis; the latter performed using the software Slope/w (Geo-Slope International Ltd.) for application of the LEM.

Findings derived from the Rinaldi et al. (2004) analysis have important implications for understanding mass failure processes in relation to the driving hydrologic variables and their dominance in the fluvial system. For example, they partly support

Figure 9.3. Seepage and stability analysis of a riverbank of the Sieve River. (Modified from Rinaldi et al. (2004)). (A) Geometry of the problem, showing finite element mesh, bank material layers (a, massive silty fine sand; b1, sand; b2, sand with cobbles included; c, silty sand; d, packed sand, gravel, and cobbles; e, loosely packed gravel and cobbles), and their properties (c' = effective cohesion; ϕ' = friction angle in terms of effective stress; ϕ^b = friction angle in terms of matric suction; γ = bulk unit weight; n = porosity; k_{sat} = saturated conductivity; n/a = data not available). (B) Results of the 14/12/1996 flow event: rainfall, river stages, groundwater levels (referred to at a constant distance of 0.5 m from the bank profile), and trend of the safety factor. (C) Minimum safety factor for the simulated flow events as a function of peak river stage: (1) single-peak hydrographs; (2) multiple-peak hydrographs. (Reproduced with permission from Wiley and Sons, 2004.)

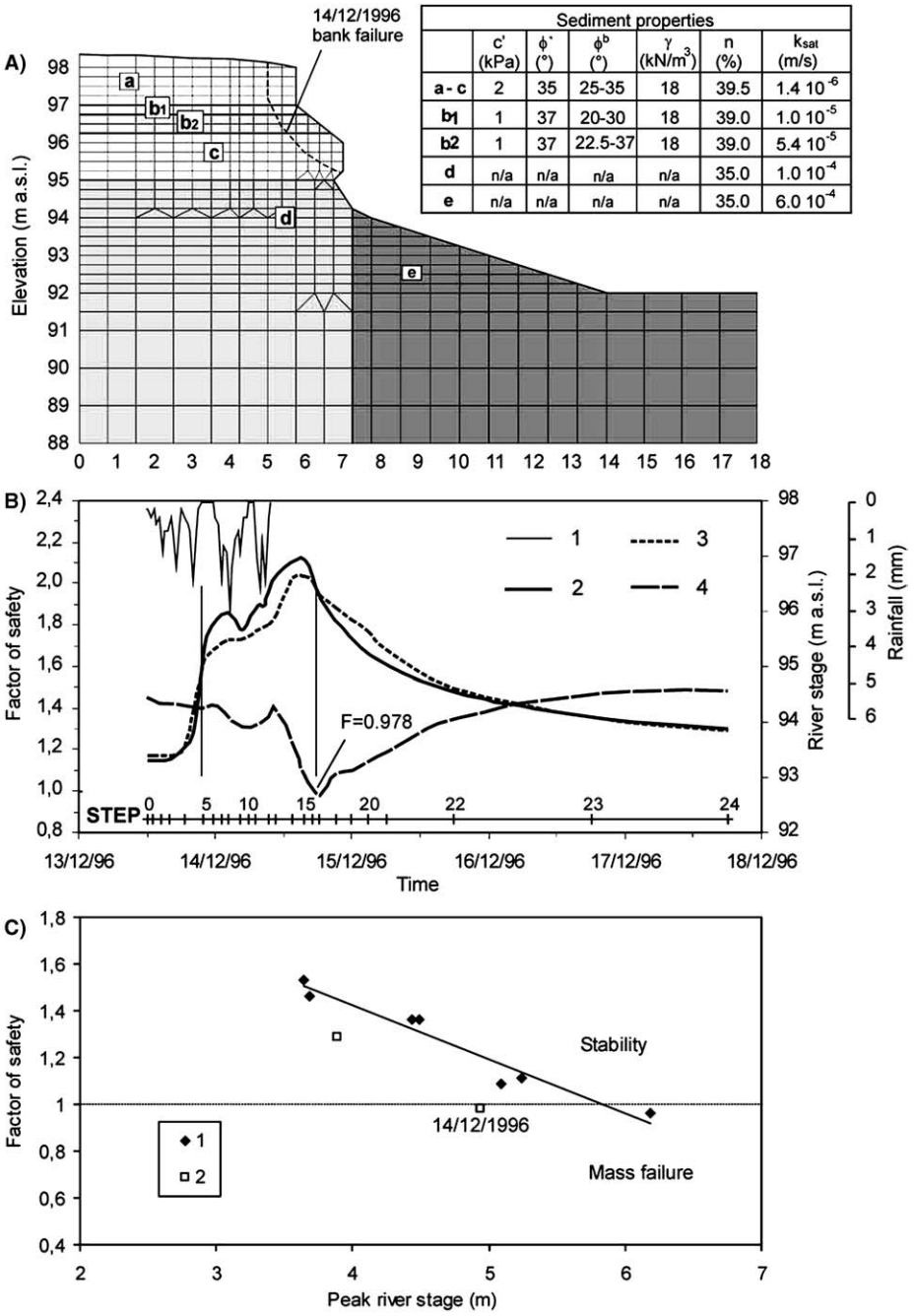

Sediment properties						
	c' (kPa)	ϕ' (°)	ϕ^b (°)	γ (kN/m^3)	n (%)	k_{sat} (m/s)
a - c	2	35	25-35	18	39.5	$1.4\ 10^{-6}$
b1	1	37	20-30	18	39.0	$1.0\ 10^{-5}$
b2	1	37	22.5-37	18	39.0	$5.4\ 10^{-5}$
d	n/a	n/a	n/a	n/a	35.0	$1.0\ 10^{-4}$
e	n/a	n/a	n/a	n/a	35.0	$6.0\ 10^{-4}$

previous authors (Thorne, 1982; Springer et al., 1985; Lawler et al., 1997b) who argued that bank failures occur primarily during the drawdown phase, but they are also better able to discriminate the details of this effect. In particular, it is evident that bank failure in this case often occurs in the very early stage of drawdown (Fig. 9.3B), due to relatively small changes in the motivating and resisting forces. Indeed, it is not necessary for the bank to be saturated to explain bank failure, as would be the case if stability was limited by 'worst case' conditions. A second implication is related to the finding that prolonged and complex hydrographs, with subsidiary peaks preceding the main one, are more destabilising than flow events with a single, distinct, rising phase (Rinaldi et al., 2004; see Fig. 9.3C). Given that the shape of the hydrograph tends to vary systematically with location in the drainage basin, it follows that different destabilising responses can be expected in different locations. In particular, the upper reaches of drainage basins are generally characterised by simple hydrographs with relatively low and distinct peaks, while the flood hydrograph generally tends to become more complex and have a longer duration in downstream reaches. Consequently, pore water pressure distributions may favour the triggering of mass failures in downstream reaches, consistent with the bank process dominance model introduced earlier (Fig. 9.2). It also follows that bank failure frequency and intensity can be promoted by climatic regimes and/or network configurations that favour multi-peaked rather than single hydrographs. A final development highlighted by Rinaldi et al. (2004) is the use of animated graphics as a means of visualising pore water dynamics, enabling the transient effects of these changes to be elucidated more clearly (e.g., 'Simulation 1' at http://www.dicea.unifi.it/massimo.rinaldi/private/simulations.htm).

Despite these recent advances, further progress is still needed to better simulate pore water pressure changes and their impacts on mass failure. One critical point is the difficulty of including in a seepage analysis those banks where the profile is undergoing deformation as a result of fluvial erosion. This is because of the need to continuously adapt the finite element mesh used to model the problem. A first attempt to address this issue has been introduced by Dapporto and Rinaldi (2003), and this is discussed in detail later.

3.3. *Effects of vegetation*

The effects of vegetation on river bank processes are many and complex, and most are difficult to quantify. A comprehensive review is beyond the immediate scope of this paper, but given that this field is one of the areas in which major recent advances in modelling bank stability have occurred, we provide a brief overview of progress made in quantifying the effects of vegetation on river bank failures.

The impacts of vegetation on mass failure can be divided into mechanical and hydrological effects, some of which are positive in terms of their impact on bank stability and some of which are negative. The net change in stability induced by vegetation is, therefore, highly contingent on site-specific factors, both in terms of the characteristics of the bank (hydrology, shape, sedimentology) and the characteristics

of the vegetation. Considering the mechanical effects of vegetation first, the net effect of vegetative surcharge can be either beneficial (increase in normal stress and therefore in the frictional component of soil shear strength) or detrimental (increasing the downslope component of gravitational force), depending on such factors as the position of the tree on the bank, the slope of the shear surface, and the friction angle of the soil (Gray, 1978; Selby, 1982). However, the most important mechanical effect that vegetation has on slope stability is the increase in soil strength induced by the presence of the root system, and considerable progress has recently been made in quantifying this effect (Gray, 1978; Wu et al., 1979; Greenway, 1987; Gray and Barker, 2004; Pollen et al., 2004; Pollen and Simon, 2005; Pollen, 2006). Surcharge and root reinforcement have been recently included in bank stability models (Abernethy and Rutherfurd, 1998, 2000, 2001; Simon and Collison, 2002; Van de Wiel and Darby, 2004; Rutherfurd and Grove, 2004; Pollen and Simon, 2005; Pollen, 2006).

In terms of the influence of riparian vegetation on local-scale river bank hydrology, three main factors can be distinguished: (a) interception; (b) infiltration; (c) evapotranspiration. Although these various hydrologic effects are well understood at a conceptual level (e.g., Greenway, 1987; Thorne, 1990), they are in practice extremely difficult to quantify and include in river bank stability models. One exception is the study of Simon and Collison (2002), who quantified the balance between potential stabilising and destabilising effects based on monitoring data from a river bank along Goodwin Creek, Mississippi (USA). A key finding of their research is that the hydrologic effects are comparable in magnitude to the mechanical effects of vegetation, and can be either beneficial or detrimental, depending on antecedent rainfall. However, the rate and amount by which plants alter the water-content distribution within a river bank depend on a great many factors related to vegetation type, soil characteristics, seasonal variations, and climatic conditions of the region. This again makes the effects of vegetation highly contingent and site-dependent, so that generalisation of results from this single study can only be attempted with extreme caution.

In addition to the complexity induced by the several and interacting effects of vegetation, a further factor limiting the reliability of prediction can also be mentioned here. Specifically, the stability of a riverbank is not only dependent on the site-specific characteristics of that bank, but it is also conditioned by channel processes operating at the reach scale. Van De Wiel and Darby (2004) have investigated this effect in a series of numerical experiments, demonstrating that reach-scale variations in bed topography induced by the presence of bank vegetation influences local river bank retreat in a spatially variable manner. The magnitude of this effect was found to be sufficiently variable that, in some circumstances, local-scale changes in bank retreat resulting from the presence of vegetation on the bank were less than the changes forced by reach-scale variations in bed topography induced by vegetation assemblages located on the banks in reaches upstream and downstream. These findings demonstrate that at-a-site analysis by itself is not always sufficient to determine the net beneficial or adverse impact on bank stability of a specific assemblage of riparian vegetation.

4. Concluding discussion: Modelling hydraulic and geotechnical interactions

The preceding sections have identified how bank retreat involves an interaction between specific erosion processes and mechanisms. Moreover, in the middle reaches of drainage basins where gravels often dominate, retreat is likely to be driven by a combination of the hydraulic forces of the flow, and mass failures driven by gravity (Fig. 9.2). This is not to exclude the importance of weathering processes, but in this conceptualisation their role is confined to providing a controlling influence on temporal variations in sediment erodibility (e.g., Prosser et al., 2000, Couper and Maddock, 2001; Lawler, 2005), such that their effect can be accounted for implicitly within fluvial-erosion models. What is clear is that for large extents of gravel-bed reaches in drainage basins, hydraulic and geotechnical factors are both significant enough that neither can be ignored (Fig. 9.2). This is not just a question of ensuring that models are comprehensive in the sense that all relevant processes are included. Rather, it is also necessary to capture the interactions between these process groups. This builds on the idea that models that incorporate complex feedbacks, non-linearities, and dynamic interactions between system components are needed to predict behaviour that would otherwise be unforeseen (e.g., Slingerland et al., 1996; Paola, 2000; Bras et al., 2003). In this section we suggest that river bank systems may also behave in this way, by modelling the interactions between hydraulic and geotechnical processes and obtaining predictions with qualitatively different outcomes (in terms of the nature of the onset and timing of bank sediment delivery to the alluvial sedimentary system) than existing models that treat these processes in isolation.

While adequate quantitative treatments that include interactions between fluvial erosion and mass failure processes are lacking, basic conceptual models are available. Specifically, Thorne (1982) has elucidated the concept of basal endpoint control as a framework for understanding the controls on riverbank retreat. The concept is based on the notion that the local bank retreat rate is determined by the status of the sediment budget at the toe of the bank, with Thorne (1982) defining three basal endpoint states as follows.

4.1. Unimpeded removal

Banks which are in dynamic equilibrium have an approximate balance between the rate at which sediment is supplied to the basal area by fluvial entrainment and mass failure and the removal of this debris by the flow.

4.2. Excess basal capacity

Here the rate of removal of sediment from the basal region exceeds the rate at which sediment is supplied to the toe, resulting toe erosion may destabilise the bank, increase the rate of retreat, and thus restore a dynamic equilibrium.

4.3. Impeded removal

Impeded removal is where bank-erosion processes supply material to the base of the bank at a higher rate than it is removed by the flow, such that deposition occurs in the basal zone. Consequently, stability with respect to mass failure increases and the rate of retreat will decrease.

The basal endpoint concept is helpful in visualising the coupling that exists between sedimentary processes operating on the banks and those operating in the channel as a whole. Also noteworthy is the point that the residence time of sediment stored at the bank toe is seen as the critical factor controlling long-term bank retreat rates. We return to the significance of this below.

4.4. A methodological framework for coupling fluvial erosion, seepage, and bank-stability models

One of the few attempts to investigate bank-erosion dynamics combining fluvial erosion, pore water pressure changes, and mass bank stability into a single, integrated, modelling approach is the work of Simon et al. (2003), who used three models (Seep/w in combination with the USDA Bank Stability and Toe Erosion (BSM) models) to simulate bank response to flow events. However, although this is undoubtedly a useful exploratory study, it is limited for the following reasons. First, and most significantly, the domain of the seepage model is not updated to account for changes in bank geometry caused by fluvial erosion. Instead, the pore water-pressure distributions are calculated for a fixed geometry prior to being imported into the BSM. Consequently, the three modelling components (fluvial erosion, seepage, and mass stability) are not fully coupled, but are instead performed independently. A second limitation of the Simon et al. (2003) study is that they employed a series of artificial, rectangular-shaped, hydrographs of specified height and duration in their simulations and it is not clear how these relate to natural flow events observed in the field.

An alternative example of a numerical simulation of river bank retreat in which fluvial erosion, seepage, and mass failure models are fully integrated is a study of bank dynamics on the Sieve River in Italy (Dapporto and Rinaldi, 2003; Darby et al., 2007). The aim of this simulation was, firstly, to test the potential of this form of integrated modelling, and secondly to quantify the contribution and mutual role that the various different processes play in controlling bank retreat. What is significant is that this research is firmly grounded in reality (recall that the Sieve River study site had been the focus of earlier bank stability research by Casagli et al., 1999 and Rinaldi et al., 2004). A representative bank profile was used to perform the simulations, using the procedure summarised in Fig. 9.4. For this study we selected a single peak flow event ($Q = 792.8\,\mathrm{m}^3/\mathrm{s}$), that occurred during 18th to 20th November, 1999. For the purposes of the seepage, erosion, and stability analyses, the flow event was discretised into a series of explicit time steps, so that the hydrograph was represented as a succession of steady-state conditions (stepped hydrograph). The time steps were not constant in duration, but were defined according to the variations

in flow and rainfall, with shorter time steps during phases of rapidly varying flow. A total number of 25 time steps was considered appropriate to represent the flow hydrograph and rainfall inputs in sufficient detail (Fig. 9.5A).

As shown in Fig. 9.4, the procedure for modelling riverbank retreat was: (i) to compute the magnitude of fluvial erosion and consequent changes in bank geometry, (ii) to determine the pore water pressure distribution via finite element seepage analysis, and (iii) to estimate the factor of safety using a slope stability analysis based on the LEM. This sequence is repeated for each subsequent time step, with the bank geometry updated in accordance with any retreat predicted by either of the fluvial erosion or mass failure analyses. Note that while each of the three modelling approaches has already been discussed individually, each requires a particular implementation within the context of the integrated simulation, and these aspects are now discussed.

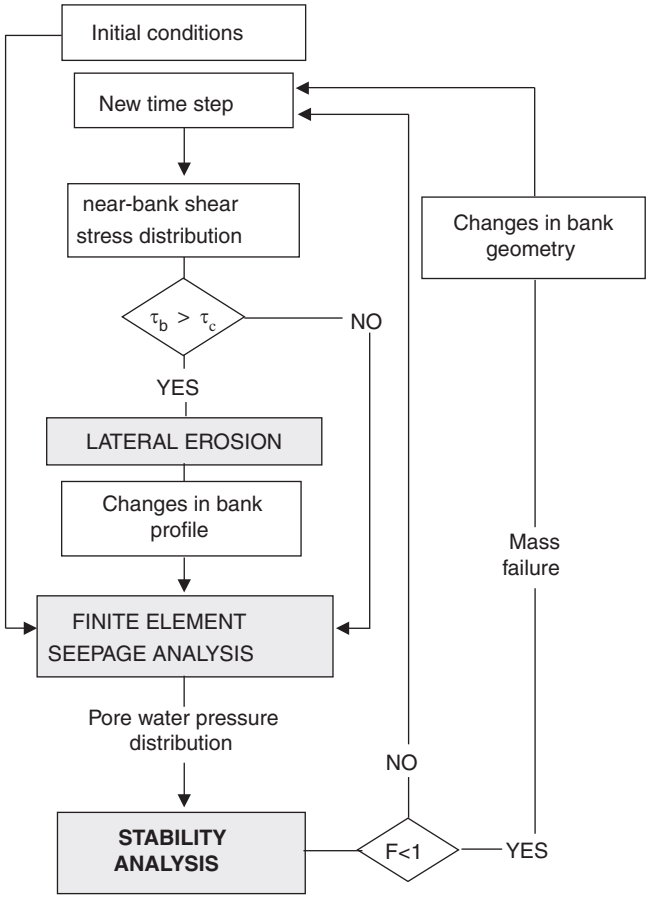

Figure 9.4. Flow chart showing the computational logic used for the coupled fluvial erosion–seepage–stability simulation of bank retreat for the 19/11/1999 bankfull event on the Sieve River, Italy.

In order to calculate increments of fluvial erosion in each time step, boundary shear stress was initially estimated using $\tau = \gamma RS$, where τ = boundary shear stress, γ = unit weight of the water, R = hydraulic radius, and S = energy slope. To transform this estimate of the mean boundary shear stress to a bank shear stress value more appropriate for modelling fluvial erosion, a distribution function derived from laboratory flume experiments for rectangular channels (Leutheusser, 1963) was used. This function was applied at each of 32 computational nodes spaced apart up the bank profile at a uniform vertical distance of 0.15 m. Admittedly, this represents a gross simplification of the actual near-bank shear stress distribution, but was used in this study merely to demonstrate the methodological approach required to combine the process models. Having obtained the bank stress, the bank profile was deformed by fluvial shear erosion estimated using equation (9.1), with different values of bank erodibility assigned to the different materials within the bank profile (Fig. 9.5B).

The finite element seepage analysis was performed by discretising the river bank profile into about 1600 quadrilateral and triangular elements, and assigning hydraulic conductivity and soil-water characteristic curves to the three layers of bank materials (Fig. 9.5B). In designing finite-element meshes used in this type of seepage analysis, the discretisation resolution must be verified to ensure that the output converges to a correct solution, independent of the grid design. The issue of grid verification has received attention in the fluid mechanics literature (e.g., Hardy et al., 2003), but to our knowledge no previous river bank study has considered this issue. The discretisation shown in Fig. 9.5B was made with the general criterion of representing the bank area close to the river border in more detail, as this is where the interactions between river stage and pore water pressures are most relevant to mass failure, and it is also where bank retreat is most likely to occur. In contrast, larger cell sizes were employed in areas more distant from the bank–river interface. Regarding the verification of this grid, we followed Hardy et al. (2003) by undertaking simulations with a range of cell sizes, confirming that the designed mesh converged to an acceptable solution.

The seepage analysis was performed for each time step but, in contrast to previous studies, the bank profile was deformed according to the magnitude of the simulated fluvial erosion. This requires special attention to adapt the finite element mesh to the new bank geometry at the end of each time step using one of two possible procedures. If the magnitude of the simulated fluvial erosion is less than the width of the boundary cell, the boundary node is shifted inwards by an amount equal to the simulated fluvial erosion. However, as cells cannot be destroyed in the seepage model, this is not possible when the fluvial-erosion increment is greater than the thickness of the boundary cell. Instead, the cell geometry is artificially modified by adjusting the hydraulic conductivity in the affected cell(s) to provide a very high transmission rate through the eroded cells (Fig. 9.5C). Subsequently the LEM was used to determine the safety factor for mass failures (for both planar slide and cantilever failure mechanisms) at the end of each time step.

Animated graphics (e.g., see 'Simulation 2' at http://www.dicea.unifi.it/massimo.rinaldi/private/simulations.htm) provide the best means of visualising the effects of the three interacting processes. However, Fig. 9.5D highlights how fluvial erosion is a quasi-continuous process, active during the entire erosive phase, whereas mass

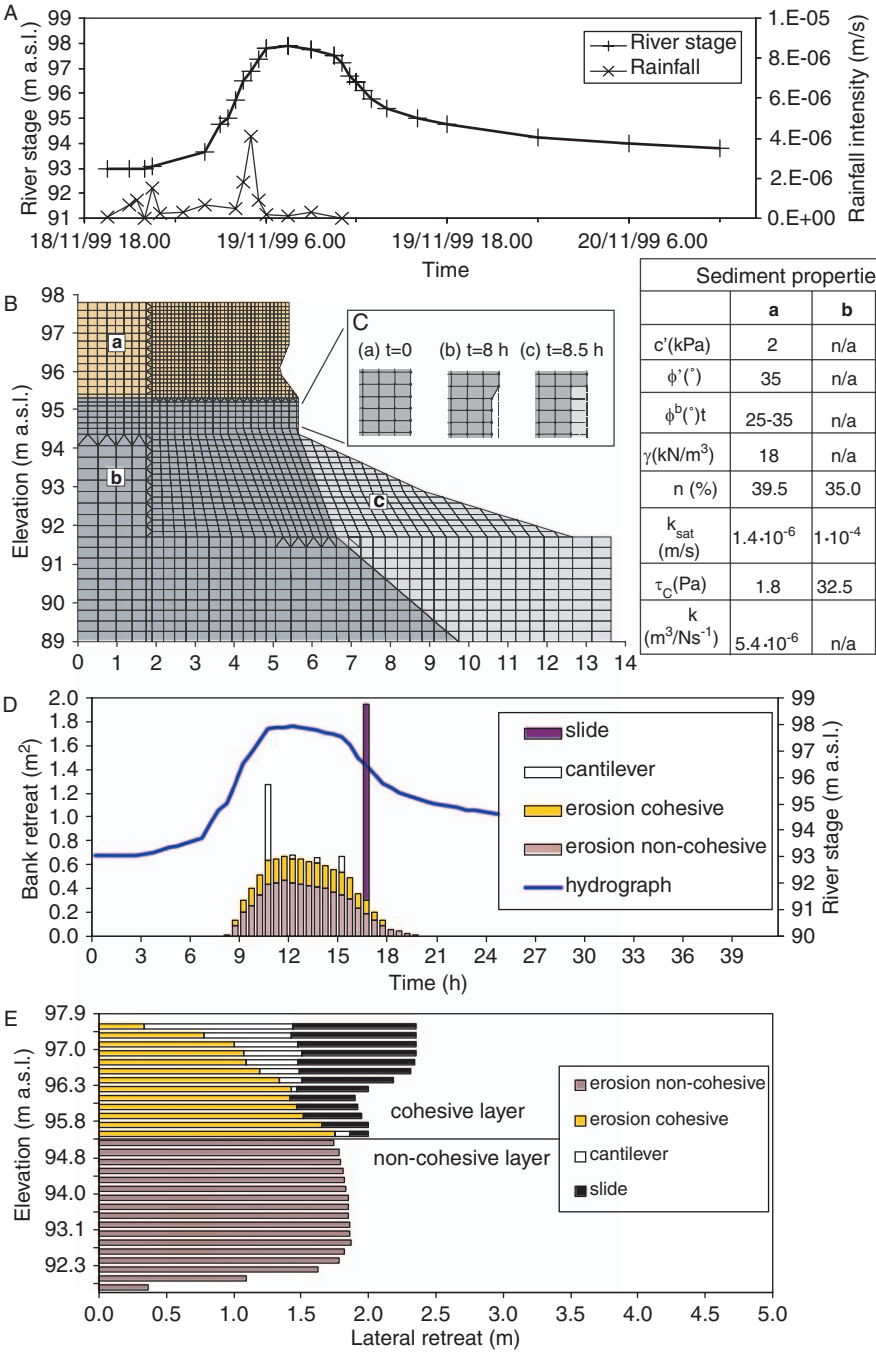

Sediment properties			
	a	**b**	**c**
c'(kPa)	2	n/a	n/a
$\phi'(^\circ)$	35	n/a	n/a
$\phi^b(^\circ)t$	25-35	n/a	n/a
$\gamma(kN/m^3)$	18	n/a	n/a
n (%)	39.5	35.0	35.0
k_{sat} (m/s)	$1.4 \cdot 10^{-6}$	$1 \cdot 10^{-4}$	$6 \cdot 10^{-4}$
τ_C(Pa)	1.8	32.5	27.9
k (m^3/Ns^{-1})	$5.4 \cdot 10^{-6}$	n/a	$2 \cdot 10^{-5}$

failures exhibit an intermittent, discontinuous behaviour, with frequent cantilever failures occurring both before and during the peak of the event, followed by a slab-rotational failure occurring during the recessional phase of the hydrograph. Fig. 9.5E shows how total retreat varies along the bank profile, thereby discriminating dominant process domains. For example, fluvial erosion is the only process responsible for the retreat of the basal granular layer, and although it is still important in the cohesive portion of the bank, mass failures dominate here. The precise mechanism of mass failure also varies with position on the bank, with the slide failure involving most of the cohesive layer, whereas cantilevers prevail on the uppermost portion of the bank.

Of particular interest is that these simulation results are qualitatively distinct from conceptual models of bank sediment delivery processes that are founded on event-scale analyses. Previous studies have tended to emphasise mass failure as a quasi-catastrophic event, typically timed to occur on the falling limb of event hydrographs. In contrast, our simulation suggests that mass failures occur as a series of erosion episodes, timed at frequent intervals (Fig. 9.6A) as progressive fluvial erosion undermines the bank and trigger failures throughout the flow event. These results can be compared with a simulation of the same flow event in which the bank profile is not deformed by fluvial erosion. For this latter case (Fig. 9.6B) only a single cantilever failure is predicted (at approximately the peak stage of the hydrograph), delivering a total unit (per metre bank length) volume of $0.35\,m^2$ of bank sediment into the channel. This is much less than the total unit volume of $11.65\,m^2$ in the deforming-profile scenario (Fig. 9.6A), of which $2.47\,m^2$ emanates from mass failures (slide and cantilevers) and $9.18\,m^2$ from fluvial erosion. Put another way, in the scenario with fluvial erosion, 7 times as much sediment is derived from mass failure and 33 times as much sediment is derived in total compared with the constant geometry case. These differences are not surprising, but they do highlight how effectively fluvial-erosion triggers mass failure. More significantly, the effect of fluvial erosion is to induce a quasi-continuous delivery of *mass-wasted* bank sediment during the early phases, and around the peak, of the flow hydrograph. This is in contrast to models that emphasise mass failure occurring on the falling limb of the hydrograph. An implication is that, even with the much greater volume of bank-derived sediment delivered in the coupled simulation, the residence time of mass-wasted debris delivered to the bank-toe may be much shorter than expected, as the material is injected into the river at times of relatively high flow, rather than on the falling limb. As a result, it seems likely that the basal endpoint status of eroding riverbanks where there is a strong

Figure 9.5. Overview of the coupled fluvial erosion–seepage–stability simulation of bank retreat for the 19/11/1999 bankfull event on the Sieve River, Italy. (A) Discretisation of the flow hydrograph; (B) geometry of the problem, showing finite element mesh, simulated bank material layers (a, massive silty fine sand; b, packed sand, gravel and cobbles; c, loosely packed gravel and cobbles), and their properties (c' = effective cohesion; ϕ' = friction angle in terms of effective stress; ϕ^b = friction angle in terms of matric suction; γ = bulk unit weight; n = porosity; k_{sat} = saturated conductivity; τ_c = critical shear stress; k_d = erodibility coefficient; n/a = data not available); (C) illustration of the procedure used to update the finite element mesh in the seepage analysis in accordance with simulated fluvial-erosion magnitudes; (D) dynamics of bank-erosion processes simulated during the flow event; (E) total contributions of the different processes to bank retreat as a function of position along the bank profile.

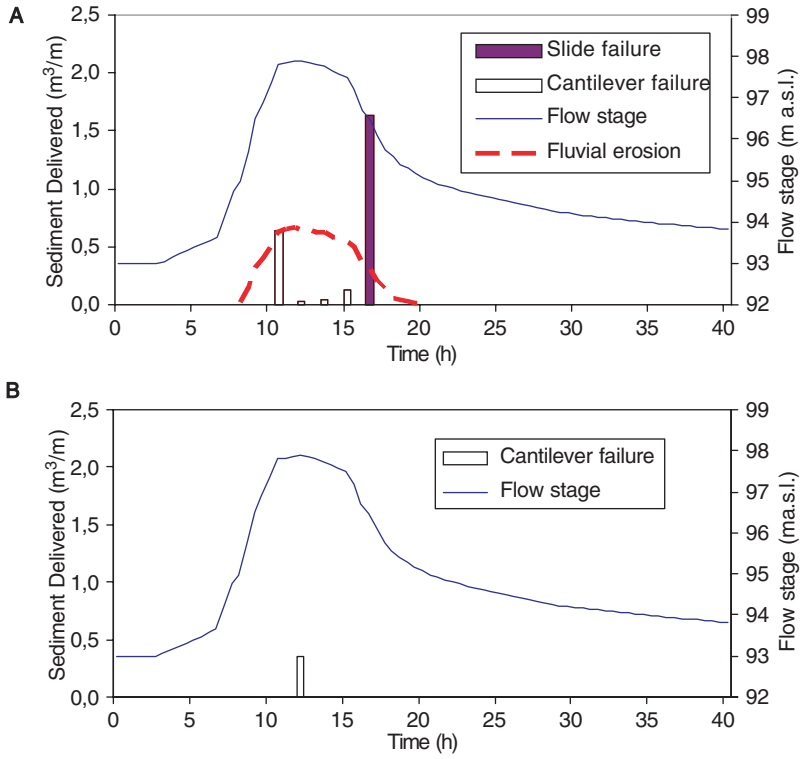

Figure 9.6. Comparison of unit sediment volumes predicted to be delivered to the channel by bank-erosion processes for the 19/11/1999 event on the Sieve River, Italy. (A) Fully coupled fluvial erosion–seepage–stability analysis; (B) 'Classical' bank stability analysis incorporating seepage processes only.

interaction between fluvial erosion and mass failure processes (Fig. 9.2) is quite distinct from riverbanks that can be represented using the 'classical' uncoupled approach. This hypothesis requires verification, but it might provide a means to explain how some rivers are able to both erode and transmit fine-grained bank sediments effectively enough to produce the very high sediment yields described in the introduction to our review.

Acknowledgements

The research reported herein was supported by a Joint Project (Ref: 15077) grant under the Royal Society's European Science Exchange Programme. Stefano Dapporto is acknowledged for his helpful support and for providing access to the results of his PhD dissertation. We also thank Colin Thorne, Richard Hardy, and two anonymous reviewers for their helpful comments on an earlier version of this paper.

References

Abernethy, B., Rutherfurd, I.D., 1998. Where along a river's length will vegetation most effectively stabilise stream banks? Geomorphology 23, 55–75.

Abernethy, B., Rutherfurd, I.D., 2000. The effect of riparian tree roots on the mass-stability of riverbanks. Earth Surf. Process. Landf. 25, 921–937.

Abernethy, B., Rutherfurd, I.D., 2001. The distribution and strength of riparian tree roots in relation to riverbank reinforcement. Hydrol. Process. 15, 63–79.

American Institute of Aeronautics and Astronautics (AIAA). 1998. Guide for the Verification and Validation of Computational Fluid Dynamics Simulations. AIAA Report G-077-1998.

American Society of Mechanical Engineers (ASME), 1993. Editorial policy on the control of numerical accuracy. J. Fluids Eng. 115, 339–340.

Amiri-Tokaldany, E., Darby, S.E., Tosswell, P., 2003. Bank stability analysis for predicting land loss and sediment yield. J. Am. Water Resour. Assoc. 39, 897–909.

Arulanandan, K., Gillogley, E., and Tully, R., 1980. Development of a quantitative method to predict critical shear stress and rate of erosion of natural undisturbed cohesive soils. Report GL-80-5, U.S. Army Engineers, Waterways Experiment Station, Vicksburg, Mississippi.

ASCE Task Committee on Hydraulics, Bank Mechanics, and Modeling of River Width Adjustment, 1998. River width adjustment. I: Processes and mechanisms. J. Hydraul. Eng. 124 (9), 881–902.

Barker, R., Dixon, L., Hooke, J., 1997. Use of terrestrial photogrammetry for monitoring and measuring bank erosion. Earth Surf. Process. Landf. 22, 1217–1227.

Blanckaert, K., Graf, W.H., 2001. Mean flow and turbulence in open-channel bend. J. Hydraul. Eng. 127, 835–847.

Bradbrook, K.F., Lane, S.N., Richards, K.S., 2000. Numerical simulation of three-dimensional, time-averaged flow structure at river channel confluences. Water Resour. Res. 36, 2731–2746.

Bras, R.L., Tucker, G.E., Teles, V., 2003. Six myths about mathematical modeling in geomorphology. In: Wilcock, P.R. and Iverson, R.M. (Eds), Prediction in Geomorphology. American Geophysical Union, Washington, DC, pp. 63–79.

Bull, L.J., 1997. Magnitude and variation in the contribution of bank erosion to the suspended sediment load of the River Severn, UK. Earth Surf. Process. Landf. 22, 1109–1123.

Casagli, N., Rinaldi, M., Gargini, A., Curini, A., 1999. Monitoring of pore water pressure and stability of streambanks: Results from an experimental site on the Sieve River, Italy. Earth Surf. Process. Landf. 24, 1095–1114.

Collison, A.J.C., 2001. The cycle of instability: Stress release and fissure flow as controls on gully head retreat. Hydrol. Process. 15, 3–12.

Couper, P.R., 2004. Space and time in river bank erosion research: A review. Area 36 (4), 387–403.

Couper, P.R., Maddock, I.P., 2001. Subaerial river bank erosion processes and their interaction with other bank erosion mechanisms on the River Arrow, Warwickshire, UK. Earth Surf. Process. Landf. 26, 631–646.

Crosato, A., 2007. Effects of smoothing and regridding in numerical meander migration models. Water Resour. Res., 43, W01401, doi:10.1029/2006WR005087.

Dapporto, S., 2001. Non-vertical jet testing of cohesive streambank toe material. School of Geography, University of Nottingham, in collaboration with USDA-ARS National Sedimentation Laboratory, Oxford, Mississippi, Internal Report, 41pp.

Dapporto, S. and Rinaldi, M., 2003. Modelling of river bank retreat by combining fluvial erosion, seepage and mass failure. Geophys. Res. Abstracts, EGS-AGU-EUG Joint Assembly, Nice, France, 6–11 April 2003.

Dapporto, S., Rinaldi, M., Casagli, N., 2001. Mechanisms of failure and pore water pressure conditions: Analysis of a riverbank along the Arno River (Central Italy). Eng. Geol. 61, 221–242.

Dapporto, S., Rinaldi, M., Casagli, N., Vannocci, P., 2003. Mechanisms of riverbank failure along the Arno River, Central Italy. Earth Surf. Process. Landf. 28 (12), 1303–1323.

Darby, S.E., Rinaldi, M., and Dapporto, S., 2007. Coupled simulations of fluvial erosion and mass wasting for cohesive riverbanks. J. Geophys. Res., 112, doi: 10.1029/2006JF000722.

Darby, S.E., Spyropoulos, M., Bressloff, N., and Rinaldi, M., 2004. Fluvial bank erosion in meanders: A CFD modelling approach. In: Garcia de Jalon Lastra, D. and Martinez, P.V. (Eds), Aquatic Habitats: Analysis and Restoration, Proceedings of the Fifth International Symposium on Ecohydraulics, September 2004, Madrid, Spain (Volume 1), International Association of Hydraulic Engineering and Research, Madrid, pp. 268–273.

Darby, S.E., Thorne, C.R., 1996a. Numerical simulation of widening and bed deformation of straight sand-bed rivers. II: Model evaluation. J. Hydraul. Eng. 122 (4), 194–202.

Darby, S.E., Thorne, C.R., 1996b. Development and testing of river-bank stability analysis. J. Hydraul. Eng. 122 (8), 443–454.

Duncan, J.M., Wright, S.G., 2005. Soil Strength and Slope StabilityWiley, 295pp.

Eaton, B.C., Church, M., Millar, R.G., 2004. Rational regime model of alluvial channel morphology and response. Earth Surf. Process. Landf. 29, 511–529.

Fredlund, D.G., Morgenstern, N.R., Widger, R.A., 1978. The shear strength of unsaturated soils. Can. Geotech. J. 15, 312–321.

Fredlund, D.G., Rahardjo, H., 1993. Soil Mechanics for Unsaturated Soils. Wiley, Chichester, 482pp.

Gerolymos, G.A., Neubauer, J., Sharma, V.C., Vallet, I., 2002. Improved prediction of turbomachinery flows using near-wall Reynolds-stress model. J. Turbomachinery 124, 86–99.

Goodson, J.M., Gurnell, A.M., Angold, P.G., Morrissey, I.P., 2002. Riparian seed banks along the lower River Dove UK – their structure and ecological implications. Geomorphology 47, 45–60.

Govers, G., 1991. Rill erosion on arable land in central Belgium: Rates, controls and predictability. Catena 18, 133–155.

Gray, D.H., 1978. Role of woody vegetation in reinforcing soils and stabilising slopes. Proc. Symp. Soil Reinforcing and Stabilising Techniques, Sydney, Australia, pp. 253–306.

Gray, D.H., Barker, D., 2004. Root–soil mechanics and interaction. In: Bennett, S.J. and Simon, A. (Eds), Riparian Vegetation and Fluvial Geomorphology. American Geophysical Union, Washington, DC, pp. 113–124.

Greenway, D.R., 1987. Vegetation and slope stability. In: Anderson, M.G. and Richards, K.S. (Eds), Slope Stability. Wiley, pp. 187–230.

Griffin, E.R., Kean, J.W., Vincent, K.R., et al., 2005. Modeling effects of bank friction and woody bank vegetation on channel flow and boundary shear stress in the Rio Puerco, New Mexico. J. Geophys. Res., 110, F04023, doi:10.1029/2005JF000322.

Griffiths, D.V., Lane, P.A., 1999. Slope stability analysis by finite elements. Geotechnique 49 (3), 387–403.

Grissinger, E.H., 1982. Bank erosion of cohesive materials. In: Hey, R.D., Bathurst, J.C., and Thorne, C.R. (Eds), Gravel-bed Rivers. Wiley, Chichester, pp. 273–287.

Hanson, G.J., 1990. Surface erodibility of earthen channels at high stresses. Part II – developing an in situ testing device. Trans. Am. Soc. Agric. Eng. 33 (1), 132–137.

Hanson, G.J., Simon, A., 2001. Erodibility of cohesive streambeds in the loess area of the midwestern USA. Hydrol. Process. 15, 23–38.

Hardy, R.J., Lane, S.N., Ferguson, R.I., Parsons, D.R., 2003. Assessing the credibility of a series of computational fluid dynamic simulations of open channel flow. Hydrol. Process. 17, 1539–1560.

Hey, R.D., Bathurst, J.C., Thorne, C.R. (Eds), 1982. Gravel-bed Rivers. Wiley, Chichester, 875pp.

Hodskinson, A., Ferguson, R., 1998. Modelling separation flow in meander bends. Hydrol. Process. 12, 1323–1338.

Hooke, J.M., 1980. Magnitude and distribution of rates of river bank erosion. Earth Surf. Process. Landf. 5, 143–157.

Howard, A.D., 1994. Badlands. In: Abrahams, A.D. and Parsons, A.J. (Eds), Geomorphology of Desert Environments. Chapman and Hall, London, pp. 213–242.

Hürlimann, M., Ledesma, A., Corominas, J., Prat, P.C., 2006. The deep-seated slope deformation at Encampadana, Andorra: Representation of morphologic features by numerical modelling. Eng. Geol. 83 (4), 343–357.

Kartha, V.C., Leutheusser, H.J., 1972. Distribution of tractive force in open channels. J. Hydraul. Div. ASCE 96, 1469–1483.

Kean, J.W., Smith, J.D., 2004. Flow and boundary shear stress in channels with woody bank vegetation. In: Bennett, S.J. and Simon, A. (Eds), Riparian Vegetation and Fluvial Geomorphology. American Geophysical Union, Washington, DC, pp. 237–252.

Kean, J.W. and Smith, J.D., 2006a. Form drag in rivers due to small-scale natural topographic features: 1. Regular sequences. J. Geophys. Res., 111, F04009, doi:10.1029/2006JF000467.

Kean, J.W. and Smith, J.D., 2006b. Form drag in rivers due to small-scale natural topographic features: 2. Irregular sequences. J. Geophys. Res., 111, F04010, doi:10.1029/2006JF000490.

Knapen, A., Poesen, J., Govers, G., et al., 2007. Resistance of soils to concentrated flow erosion: A review. Earth Sci. Rev. 80, 75–109.

Knight, D., Demetriou, J.D., Hamed, M.E., 1984. Boundary shear in smooth rectangular channels. J. Hydraul. Eng. 110, 405–422.

Lane, E.W., 1955. Design of stable channels. Trans. Am. Soc. Civil Eng. 120, 1–34.

Lane, S.N., Bradbrook, K.F., Richards, K.S., et al., 2000. Secondary circulation cells in river channel confluences: Measurement artefacts or coherent flow structures. Hydrol. Process. 14, 2047–2071.

Lane, S.N., Chandler, J.H., Richards, K.S., 1994. Developments in monitoring and terrain modelling small-scale river-bed topography. Earth Surf. Process. Landf. 19, 349–368.

Lawler, D.M., 1992. Process dominance in bank erosion systems. In: Carling, P.A. and Petts, G.E. (Eds), Lowland Floodplain Rivers: Geomorphological Perspectives. Wiley, pp. 117–143.

Lawler, D.M., 1993. The measurement of river bank erosion and lateral channel change. Earth Surf. Process. Landf. 18, 777–821.

Lawler, D.M., 2005. Defining the moment of erosion: The principle of thermal consonance timing. Earth Surf. Process. Landf. 30(13), 1597–1615.

Lawler, D.M., Bull., L., Harris, N.M., 1997a. Bank erosion events and processes in the Upper Severn. Hydrol. Earth System Sci. 1, 523–534.

Lawler, D.M., Thorne, C.R., Hooke, J.M., 1997b. Bank erosion and instability. In: Thorne, C.R., Hey, R.D., and Newson, M.D. (Eds), Applied Fluvial Geomorphology for River Engineering and Management. Wiley, Chichester, pp. 137–172.

Leutheusser, H.J., 1963. Turbulent flow in rectangular ducts. Proc. Am. Soc. Civil Eng. 89, HY3.

Lohnes, R., Handy, R.L., 1968. Slope angles in friable loess. J. Geol. 76, 247–258.

Millar, R.G., 2000. Influence of bank vegetation on alluvial Channel patterns. Water Resour. Res. 36 (4), 1109–1118.

Millar, R.G., Quick, M.C., 1993. Effect of bank stability on geometry of gravel rivers. J. Hydraul. Eng. 119, 1343–1363.

Nagihara, S., Mulligan, K.R., Xiong, W., 2004. Use of a three-dimensional laser scanner to digitally capture the topography of sand dunes in high spatial resolution. Earth Surf. Process. Landf. 29, 391–398.

Nicholas, A.P., Sambrook-Smith, G.H., 1999. Numerical simulation of three-dimensional flow hydraulics in a braided channel. Hydrol. Process. 13, 913–929.

Nicholas, A.P., Walling, D.E., 1997. Modelling flood hydraulics and overbank deposition on river floodplains. Earth Surf. Process. Landf. 22, 59–77.

Nicholas, A.P., Walling, D.E., 1998. Numerical modelling of floodplain hydraulics and suspended sediment transport and deposition. Hydrol. Process. 12, 1339–1355.

Osman, A.M., Thorne, C.R., 1998. Riverbank stability analysis. Part I: Theory. J. Hydraul Div. ASCE 114 (2), 125–150.

Paola, C., 2000. Quantitative models of sedimentary basin filling. Sedimentology 47, 121–178.

Partheniades, E., 1965. Erosion and depostion of cohesive soils. J. Hydraul. Div. ASCE 91, 105–139.

Pollen, N., 2006. Temporal and spatial variability of root reinforcement of streambanks: Accounting for soil shear strength and moisture. Catena 69, doi:10.1016/j.catena.2006.05.004.

Pollen, N. and Simon, A., 2005. Estimating the mechanical effects of riparian vegetation on streambank stability using a fiber bundle model. Water Resour. Res. 41, W07025. doi:10.1029/2004WR003801

Pollen, N., Simon, A., Collison, A., 2004. Advances in assessing the mechanical and hydrologic effects of riparian vegetation on streambank stability. In: Bennett, S.J. and Simon, A. (Eds), Riparian Vegetation and Fluvial Geomorphology. American Geophysical Union, Washington, DC, pp. 125–140.

Prosser, I.P., Hughes, A.O., Rutherfurd, I.D., 2000. Bank erosion of an incised upland channel by subaerial processes: Tasmania, Australia. Earth Surf. Process. Landf. 25, 1085–1101.

Reneau, S.L., Drakos, P.G., Katzman, D., et al., 2004. Geomorphic controls on contaminant distribution along an ephemeral stream. Earth Surf. Process. Landf. 29, 1209–1223.

Rinaldi, M., Casagli, N., 1999. Stability of streambanks formed in partially saturated soils and effects of negative pore water pressures: The Sieve River (Italy). Geomorphology 26 (4), 253–277.

Rinaldi, M., Casagli, N., Dapporto, S., Gargini, A., 2004. Monitoring and modelling of pore water pressure changes and riverbank stability during flow events. Earth Surf. Process. Landf. 29 (2), 237–254.

Rinaldi, M., Dapporto, S., Casagli, N., 2001. Monitoring and modelling of unsaturated flow and mechanisms of riverbank failure in gravel bed rivers. In: Nolan, T. and Thorne, C.R. (Eds), Gravel Bed Rivers 2000 CD-ROM. Special Publication of the New Zealand Hydrological Society.

Rodi, W., Ferziger, J.H., Breuer, M., Pourquie, M., 1997. Status of large eddy simulation: Results of a workshop. J. Fluids Eng. 119, 248–261.

Rutherfurd, I.D., Grove, J.R., 2004. The influence of trees on stream bank erosion: Evidence from root-plate abutments. In: Bennett, S.J. and Simon, A. (Eds), Riparian Vegetation and Fluvial Geomorphology. American Geophysical Union, Washington, DC, pp. 141–152.

Selby, M.J., 1982. Hillslope Materials and Processes. Oxford University Press, Oxford, UK.

Simon, A., 1995. Adjustment and recovery of unstable alluvial channels: Identification and approaches for engineering management. Earth Surf. Process. Landf. 20, 611–628.

Simon, A., Collison, A., 2002. Quantifying the mechanical and hydrologic effects of riparian vegetation on streambank stability. Earth Surf. Process. Landf. 27, 527–546.

Simon, A., Curini, A., Darby, S.E., Langendoen, E.J., 2000. Bank and near-bank processes in an incised channel. Geomorphology 35, 193–217.

Simon, A., Darby, S.E., 2002. Effectiveness of grade-control structures in reducing erosion along incised river channels: The case of Hotophia Creek, Mississippi. Geomorphology 42, 229–254.

Simon, A., Langendoen, E.J., Collison, A., and Layzell, A., 2003. Incorporating bank-toe erosion by hydraulic shear into a bank-stability model: Missouri River, Eastern Montana. Proceedings, EWRL-ASCE, World Water and Environmental Resources Congress, Cd-Rom, 11.

Simon, A., Thomas, R.E., Curini, A., Shields, F.D. Jr., 2002. Case study: Channel stability of the Missouri River, Eastern Montana. J. Hydraul. Eng. 128 (10), 880–890.

Simon, A., Wolfe, W.J., and Molinas, A., 1991. Mass-wasting algorithms in an alluvial channel model. Proceedings of the 5th Federal Interagency Sedimentation Conference, Las Vegas, Nevada, 2, 8–22 to 8–29.

Simons, D.B., Sentürk, F., 1977. Sediment Transport Technology. Water Resources Publications, Fort Collins, CO.

Slingerland, R.L., Kump, L.R., Arthur, M.A., Barron, E.J., 1996. Estuarine circulation in the Turonian Western Interior Seaway of North America. Geol. Soc. Am. Bull. 108, 941–952.

So, R.M.C., Speziale, C.G., Launder, B.E., 1993. Near-Wall Turbulent Flows. Elsevier, New York.

Sotiropoulos, F., 2001. Progress in modelling 3D shear flows using RANS equations and advanced turbulence closures. In: Tzabiras, G.D. (Ed.), Calculation of Complex Turbulent Flows, Advances in Fluid Mechanics Series. WIT Press, Southampton, pp. 209–248.

Springer, F.M. Jr., Ullrich, C.R., Hagerty, D.J., 1985. Streambank stability. J. Geotech. Eng. 111 (5), 624–640.

Thorne, C.R., 1982. Processes and mechanisms of river bank erosion. In: Hey, R.D., Bathurst, J.C., and Thorne, C.R. (Eds), Gravel-bed Rivers. Wiley, Chichester, pp. 227–271.

Thorne, C.R., 1990. Effects of vegetation on riverbank erosion and stability. In: Thornes, J.B. (Ed.), Vegetation and Erosion. Wiley, pp. 125–144.

Thorne, C.R., Abt, S.R., 1993. Analysis of riverbank instability due to toe scour and lateral erosion. Earth Surf. Process. Landf. 18, 835–843.

Thorne, C.R., Murphey, J.B., and Little, W.C., 1981. Bank stability and bank material properties in the bluffline streams of northwest Mississippi. Appendix D. Report to the U.S. Army Corps of Engineers, Vicksburg District Office, on Stream Channel Stability, 258pp.

Thorne, C.R., Tovey, N.K., 1981. Stability of composite river banks. Earth Surf. Process. Landf. 6, 469–484.

Thorne, S.D., Furbish, D.J., 1995. Influences of coarse bank roughness on flow within a sharply curved river bend. Geomorphology 12, 241–257.

Tolhurst, T.J., Black, K.S., Shayler, S.A., et al., 1999. Measuring the in situ erosion shear strength of intertidal sediments with the Cohesive Strength Meter (CSM). Estuarine, Coastal Shelf Sci. 49, 281–294.

Van De Wiel, M.J., Darby, S.E., 2004. Numerical modeling of bed topography and bank erosion along tree-lined meandering rivers. In: Bennett, S.J. and Simon, A. (Eds), Riparian Vegetation and Fluvial Geomorphology. American Geophysical Union, Washington, DC, pp. 267–282.

Van Eerdt, M.M., 1985. Salt marsh cliff stability in the Oosterschelde. Earth Surf. Process. Landf. 10, 95–106.

Walling, D.E., Owens, P.N., Leeks, G.J.L., 1999. Fingerprinting suspended sediment sources in the catchment of the River Ouse, Yorkshire, UK. Hydrol. Process. 13, 955–975.

Wiberg, N.E., Koponen, M., Runesson, K., 2005. Finite element analysis of progressive failure in long slopes. Int. J. Numer. Anal. Met. 14 (9), 599–612.

Wu, T.H., McKinnell, W.P., Swanston, D.N., 1979. Strength of tree roots and landslides on Prince of Wales Island, Alaska. Can. Geotech. J. 16 (1), 19–33.

Discussion by Gary Williams

The bank-erosion model has been based on an actual river bank. Presumably actual bank retreat was measured for a given rainfall and flood hydrograph. How was the erosion model calibrated against actual bank retreat? What was adjusted to fit, and why was that adjustment approach used?

Reply by the authors

In the erosion model, the erodibility coefficient of the basal packed gravel is the calibration parameter, being defined by forcing best agreement between calculated and measured final bank toe retreat at the end of the simulation. This is done because reliable methods for measuring erodibility parameters for the packed gravel are not available.